Chapter 4
Sparsity-Promoting Solution of Subsurface Flow Model Calibration Inverse Problems

Behnam Jafarpour

Abstract Identification of heterogeneous hydraulic aquifer properties from limited dynamic flow measurements typically leads to underdetermined nonlinear inverse problems that can have many solutions, including solutions that are geologically implausible and fail to predict future performance of the system. The problem is usually regularized by incorporating implicit or explicit prior information to stabilize the solution techniques and to obtain plausible solutions. A meaningful regularization must be informed by the physics of the problem, distinct properties of the formation under investigation, and other available sources of information (e.g., outcrop, well logs, and seismic). This chapter proposes sparsity as an intrinsic property of spatially distributed aquifer hydraulic properties that can be used to regularize the solution of the related ill-posed inverse problem. Inspired by recent advances in *sparse* signal processing, formalized under the *compressed sensing* paradigm, proper sparsifying bases are introduced to describe aquifer hydraulic conductivity distribution. Such descriptions give rise to a sparse reconstruction formulation of the subsurface flow model calibration inverse problem, which can be efficiently solved following recent algorithmic developments in sparse signal processing. The compressed sensing paradigm specifies the conditions under which unique solutions to underdetermined linear system of equations exist and can be computed efficiently. Sparsity is a fundamental notion in compressed sensing, and is often present in many natural images. In particular, sparsity is prevalent in describing many spatially correlated aquifer properties. The practical implications of compressed sensing are as far reaching as the solution of underdetermined system of equations is in science and engineering. This chapter introduces the guidelines set

B. Jafarpour (✉)
Department of Chemical Engineering and Materials Science, University of Southern California, 925 Bloom Walk, HED 313 Los Angeles, CA 90089-1211, USA
e-mail: behnam.jafarpour@usc.edu

P.K. Mishra and K.L. Kuhlman (eds.), *Advances in Hydrogeology*,
DOI 10.1007/978-1-4614-6479-2_4,

forth by sparse reconstruction techniques and the compressed sensing paradigm and incorporates them to formulate and solve ill-posed groundwater model calibration inverse problems.

4.1 Groundwater Model Calibration

Development of underground hydrological, environmental, and energy resources relies on accurate modeling and prediction of fluid flow and transport in these heterogeneous and anisotropic porous environments. However, understanding subsurface physical, chemical, and biological rock properties and the related transport processes is severely complicated by our inability to "see into the earth". Determination of rock hydraulic properties and the underlying flow and transport processes inherently involves significant uncertainty because we can neither observe nor easily access these properties from the surface (National Research Council 2000; Yeh et al. 2008). Data limitation results in extensive interpolation and interpretation efforts that lead to the introduction of a significant level of uncertainty and bias in characterizing subsurface flow property distributions.

To reduce the uncertainty in describing the subsurface flow and transport properties, it is common to calibrate subsurface models against dynamic performance data such as pressure and flow rates. Model calibration is accomplished by formulating and solving an inverse problem where limited dynamic data is used to infer a large number of unknown parameters. Since the number of unknowns to identify is often overwhelmingly greater than the available data, the resulting inverse problems tend to be severely ill-posed and have non-unique solutions. In general, however, the true dimensionality of subsurface flow and transport models is far less than the size of the discretized numerical models used to describe them. This is attributed to the intrinsic geologic continuity that leads to extensive spatial correlations in the rock physical property distributions. An obvious way to improve the solution of ill-posed inverse problems is to collect more independent data. However, data acquisition is an expensive endeavor that is limited by economic constraints. In addition to increasing the data, advanced computational tools may be used to reduce the number of unknown parameters in the model calibration inverse problem. Several explicit and implicit parameter reduction (parameterization) techniques are available to perform this. In this chapter, a novel model calibration approach is proposed based on recent developments in sparse signal processing and approximation theory, formalized as the *compressed sensing* paradigm (Donoho 2006).

4.1.1 Flow Equations and Inverse Modeling Formulation

Mathematical modeling of multiphase fluid flow in porous media is widely used to quantify and predict fluid displacement patterns in the subsurface environment.

The general form of the governing equations for two-phase immiscible flow in porous media can be derived from the mass conservation principle and Darcy's law as (Aziz and Settari 1979; Bear and Verruijt 1987)

$$\begin{aligned}\nabla\cdot\left(\frac{\lambda_w}{B_w}u\left(\nabla P_w-\gamma_w\nabla Z\right)\right)&=\frac{\partial}{\partial t}\left(\phi\frac{S_w}{B_w}\right)+q_w\\ \nabla\cdot\left(\frac{\lambda_n}{B_n}u\left(\nabla P_n-\gamma_n\nabla Z\right)\right)&=\frac{\partial}{\partial t}\left(\phi\frac{S_n}{B_n}\right)+q_n,\end{aligned}\tag{4.1}$$

where subscripts w and n indicate wetting and non-wetting phases, λ represents the phase mobility, B the volume of a phase as a function of pressure relative to its volume at standard pressure, u the intrinsic permeability, ϕ the porosity of the medium as a function in space, P the phase pressure, γ the phase density, Z the gravity potential, S the phase saturation, and q sink and source fluxes.

The partial differential equations (PDEs) in (4.1) contain four unknown state variables, i.e., P_w, P_n, S_w, S_n. For a given set of model inputs, the system is closed by the following two constitutive equations that account for capillary pressure and the physical saturation constraint in a fully saturated medium:

$$\begin{aligned}P_n-P_w&=P_c\left(S_w\right)\\ S_n+S_w&=1.\end{aligned}\tag{4.2}$$

Forward integration of Eqs. (4.1) and (4.2) is used to compute pressure and saturation solutions in time, as a function of model inputs.

Solutions to (4.1) and (4.2) are only reliable and meaningful when accurate model inputs are used. Since direct measurement of rock hydraulic properties is difficult, we frequently need to estimate these parameters by inverting scattered point measurements and indirect data. An estimate for the unknown parameter vector $\mathbf{u}$ can be obtained by minimizing a suitable objective function, such as

$$\begin{aligned}&\min_{\mathbf{u}\in\mathcal{R}^N}J\left(\mathbf{u}\right)=\left(\mathbf{d}_{\text{obs}}-\mathbf{g}\left(\mathbf{u}\right)\right)^{\mathrm{T}}\mathbf{C}_{\mathbf{d}}^{-1}\left(\mathbf{d}_{\text{obs}}-\mathbf{g}\left(\mathbf{u}\right)\right)+Reg\left(\mathbf{u}\right)\\ &\quad s.t.\quad \mathbf{f}\left(\mathbf{u},\mathbf{x}(\mathbf{u}),\mathbf{z}\right)=0.\end{aligned}\tag{4.3}$$

Here, J is the objective function, $\mathbf{u}$ denotes the unknown parameters such as permeability, $\mathbf{d}_{\text{obs}}$ represents a vector of observed quantities, $\mathbf{g}\left(\mathbf{u}\right)$ is the predicted observations, $\mathbf{C}_{\mathbf{d}}$ refers to the covariance of measurement errors, $\mathbf{f}$ is a constraint vector containing the conservation Eqs. (4.1) and (4.2), $\mathbf{x}(\mathbf{u})$ refers to the dependent state variables, and $\mathbf{z}$ represents a vector containing other known model input parameters. Note that in the above notation, $\left\|\mathbf{d}_{\text{obs}}-\mathbf{g}\left(\mathbf{u}\right)\right\|_{\mathbf{C}_{\mathbf{d}}^{-1}}^{2}=\left(\mathbf{d}_{\text{obs}}-\mathbf{g}\left(\mathbf{u}\right)\right)^{\mathrm{T}}\mathbf{C}_{\mathbf{d}}^{-1}\left(\mathbf{d}_{\text{obs}}-\mathbf{g}\left(\mathbf{u}\right)\right)$, and the term $Reg\left(\mathbf{u}\right)$ is used to represent a general regularization term that will be discussed later. A major issue encountered when solving the resulting inverse problem is the choice of parameterization. The standard grid-based descriptions for the unknown field $\mathbf{u}$ often result in ill-posed inverse

problems that have more unknowns than can be uniquely estimated from available data. As a result, multiple solutions can be found that reproduce the observed flow and pressure data but provide different predictions of the flow and transport behavior in the future. In the last decade, however, significant progress has been made in conditioning numerical groundwater and hydrocarbon reservoir models to flow and transport data (see Kitanidis and Vomvoris 1983; McLaughlin and Townley 1996; Carrera et al. 2005; Hill and Tiedeman 2007; Oliver et al. 2008). Deterministic and stochastic inversion algorithms with varying levels of complexity have been developed and applied to solve subsurface flow inverse problems. Two common approaches for mitigating instability and non-uniqueness issues in solving ill-posed inverse problems are (a) reducing the number of unknown parameters, i.e., parameterization (e.g., Jacquard and Jain 1965; Doherty 2003; Gavalas et al. 1976), and (b) incorporating prior information in the form of constraints, i.e., regularization (e.g., Tikhonov and Arsenin 1977; Tonkin and Doherty 2005; Hill and Tiedeman 2007; Oliver et al. 2008).

4.1.2 Parameterization and Regularization

Parameterization methods can be broadly classified into spatial and transform-domain methods. Spatial parameterization methods were introduced to subsurface inverse modeling as early as 1965 in the form of zonation (Jacquard and Jain 1965) and have evolved into adaptive multiscale estimation methods (e.g., Chavent and Bissell 1998; Grimstad et al. 2003; Aanonsen 2008). The general objective of this approach is to identify spatial regions (zones) in the aquifer model that can be aggregated and assigned a single constant property value for the inversion purpose. The main difficulties in implementing zonation are related to the identification of zones with similar properties and the non-geologic sudden discontinuities at the boundaries of the identified regions. Transform-domain parameterization methods reduce the redundancy in grid-based property descriptions by recognizing that geologic features exhibit strong spatial correlations. Hence, adopting high-resolution grid-based spatial descriptions for inverse modeling is inefficient since the goal is to estimate spatially correlated geologic features from low-resolution flow data. Several transform-domain parameterization techniques have been applied to subsurface flow and transport inverse problems including principle component analysis (PCA) (Gavalas et al. 1976), discrete cosine transform (DCT) (Ahmed et al. 1974; Jafarpour and McLaughlin 2009a,b), and discrete wavelet transform (DWT) (Mallat 2008; Jafarpour et al. 2010; Sahni and Horne 2005). These methods attempt to provide a compact representation of the parameters to substantially reduce the number of unknowns in the inverse problem. A key issue in implementing these techniques is identifying the significant basis components that explain the main variability in the parameter fields. This issue has been elegantly addressed by the recent developments in sparse signal processing, which is the central topic of this chapter.

Regularization of ill-posed subsurface inverse problems can also be carried out by constraining the solution to honor explicit prior models, available static data, and/or some global attributes of the parameter field such as smoothness (e.g., Tikhonov and Arsenin 1977; Constable et al. 1987; Tonkin and Doherty 2005). In general, regularization serves two primary purposes: it (a) stabilizes the solution of an ill-posed inverse problem and (b) constrains the solution to adequately reproduce the observed data without generating unjustifiably complex artifacts (Constable et al. 1987). By using prior information about the parameters, directly or indirectly, regularization is applied to mathematically improve the behavior of the inverse modeling objective function and/or implicitly reduce the dimensionality of the parameter search space. Several regularization methods with varying levels of sophistication have been applied to subsurface characterization inverse problems (e.g., Tikhonov and Arsenin 1977; Portniaguine and Zhdanov 1999; Tonkin and Doherty 2005; Hill and Tiedeman 2007; Oliver et al. 2008). In some cases (Jafarpour et al. 2010), a combination of parameterization and regularization may prove more effective as certain solution attributes (e.g., sparsity) may only be realized and effectively exploited in a properly selected transform domain. An instance of this combined case is discussed in more detail next. To motivate the use of sparse reconstruction for model calibration, the fundamental concept and practical implications of compressed sensing paradigm are briefly introduced first, followed by a simple illustrative example.

4.2 Sparse Reconstruction and Compressed Sensing

Consider the problem of solving the system of equations $\mathbf{\Phi v} = \mathbf{u}$, where $\mathbf{\Phi} \in \mathbb{R}^{M \times N}$. In many realistic applications $M \ll N$, rendering the problem severely underdetermined. From classical linear algebra for $M < N$, this system of equations does not yield a unique solution. When the solution vector $\mathbf{v}$ is known to be sparse (i.e., many of its components are zero), however, one may hope to find a unique solution by taking advantage of the knowledge about the solution sparsity. This situation is illustrated with a simple example in Fig. 4.1. In this figure, an underdetermined linear system of equations with $M = 4$ equations and $N = 20$ unknowns is sketched. In this case, the true solution vector $\mathbf{v}$ has only $S = 4$ nonzero components. Without exact knowledge of its sparsity (i.e., the number and location of its nonzero elements), $\mathbf{v}$ cannot be identified from the available measurements. As shown on the bottom part of Fig. 4.1, if the sparsity structure of the solution $\mathbf{v}$ is perfectly known in advance, the system can be reduced to an even-determined $M = N = 4$ linear system of equations. For many sparse vectors, an apparently underdetermined problem often may be reduced to an (even-) overdetermined problem if the sparsity structure is known. However, in reality, exact a priori knowledge about the sparsity structure in the solution is not available. That is, while it may be known that a given problem is likely to have sparse solutions, the exact sparsity structure is usually unknown. When the solution is sufficiently

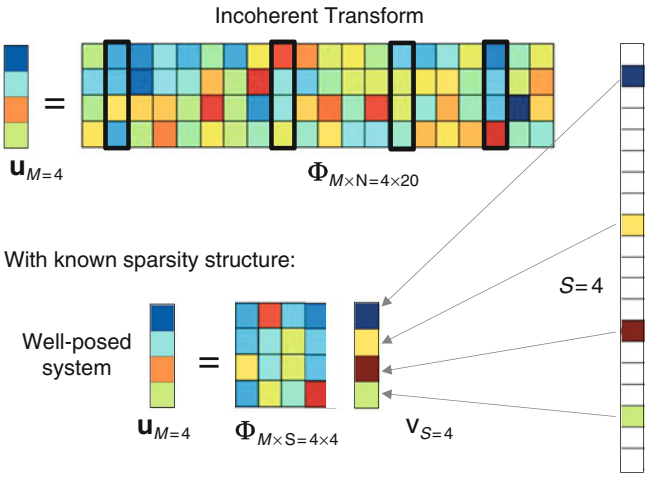

Fig. 4.1 Schematic illustration of how knowledge of solution sparsity can lead to finding a unique solution of underdetermined linear system of equations: a key unknown is the sparsity structure, which must be estimated along with the value of the nonzero (active) elements

sparse, with increasing number of independent measurements, it is less likely to find solutions that are sparser than the true solution and that satisfy the measurement constraints. In the limit, as the number of independent measurements exceeds a certain threshold, the true solution becomes the sparsest solution that satisfies the linear measurement equations. *Compressed sensing* (Donoho 2006) formalizes the conditions under which unique solutions to sparse underdetermined linear systems of equations exist and can be computed efficiently. A general approach to finding a sparse solution to $\mathbf{\Phi v} = \mathbf{u}$ is to formulate and solve a minimization problem of the form

$$(P_J): \quad \min_{\mathbf{v}} J(\mathbf{v}) \quad s.t. \quad \mathbf{u} = \mathbf{\Phi v} \tag{4.4}$$

in which $J(\mathbf{v})$ promotes solution sparsity. A good choice for $J(\mathbf{v})$ is the number of nonzero elements of the solution vector $\mathbf{v}$. This leads to the sparse reconstruction problem

$$(P_0): \quad \min_{\mathbf{v}} \|\mathbf{v}\|_0 \quad s.t. \quad \mathbf{u} = \mathbf{\Phi v}, \tag{4.5}$$

where $\|\mathbf{v}\|_0$ counts the number of nonzero components of $\mathbf{v}$. Solving (P_0) leads to a combinatorial problem that requires an exhaustive search over all possible sparse subsets of $\mathbf{v}$, which is NP-hard (Natarajan 1995). There is a vast literature concerned with finding a reliable, efficient, and robust solution approach to (P_0). It can be shown (Donoho and Elad 2003) that a solution $\mathbf{v}$ with the number of nonzero entries

$$\|\mathbf{v}\|_0 < \frac{1}{2}\left(1 + \frac{1}{\mu(\mathbf{\Phi})}\right), \tag{4.6}$$

where

$$\mu(\mathbf{\Phi}) = \min_{1 \le k,j, \le m, k \ne j} \frac{\left|\phi_k^{\mathrm{T}} \phi_j\right|}{\|\phi_k\|_2 \left\|\phi_j\right\|_2} \tag{4.7}$$

is the mutual coherence of $\mathbf{\Phi}$ and ϕ_j is the jth column of $\mathbf{\Phi}$, is necessarily the sparsest solution.

From Eqs. (4.6) and (4.7), the (nearly) orthogonal sensing matrix $\mathbf{\Phi}$ has low mutual coherence; thus, the solution of ℓ_p-norm optimization ($p \le 1$) is equivalent to that of ℓ_0-norm optimization. Examples of sparse sampling matrices with low mutual coherence that are frequently used in sparse reconstruction literature are the Gaussian and Bernoulli random matrices. Compressive bases such as DCT and DWT also have incoherent columns and are examples of possible candidates for sparse reconstruction.

Efficient approximate solutions known as *pursuit algorithms* have been developed to solve (P_0). The main practical algorithms are classified as the *greedy algorithms* (GA), also known as *matching pursuit* (MP) (Tropp and Gilbert 2007; Mallat and Zhang 1993; Couvreur and Bresler 2000), and the *convex relaxation* techniques (Santosa and Symes 1986; Chen et al. 1998; Rao and Kreutz-Delgado 2003; Karlovitz 1970; Gorodnitsky and Rao 1997). A *greedy* strategy for finding a solution is to avoid the exhaustive combinatorial search by taking locally optimal steps (Tropp and Gilbert 2007). In this approach, starting with an initially empty matrix and $\mathbf{v}^0 = 0$, iterative construction of a k-term approximation $\mathbf{v}^k$ is obtained by maintaining a set of active columns and adding an additional column at each step. The added column is chosen to maximally reduce the residual ℓ_2 error in approximating $\mathbf{u}$ with currently active columns (Tropp and Gilbert 2007). This procedure is continued until a stopping criterion, usually an error threshold, is reached. The computational complexity of the above greedy algorithm is significantly better than an exhaustive search; however, the variants of this method mainly suffer from a lack of robustness and guaranteed convergence to a sparse solution.

Convex relaxation methods (Chen et al. 1998; Donoho 2006) try to make the problem more tractable by replacing the highly discontinuous ℓ_0-norm with a more continuous sparsity-promoting penalty function. The ℓ_p-norm, i.e., $J(\mathbf{v}) = \|\mathbf{v}\|_p = (\sum_{i=1}^{N} |v_i|^p)^{\frac{1}{p}}$, with $p \in (0,1]$, and $J(\mathbf{v}) = \sum_j v_j^2 / \left(\beta^2 + v_j^2\right)$, with $\beta \to 0$ (referred to as compactness constraint), are possible choices that behave similarly to the ℓ_p-norm, for small p values (see Fig. 4.2). When the ℓ_p-norm with $p \in (0,1]$ is used to promote sparsity, a popular class of approximate algorithms to find a solution is the iteratively reweighted least-squares (IRLS) technique (Chartrand and Yin 2008). Note that although for $p < 1$ the norm definition is violated, the term ℓ_p-norm is commonly used in the literature.

For $p = 1$, the problem reduces to a convex optimization problem of the form

$$(P_1): \quad \min_{\mathbf{v}} \|\mathbf{v}\|_1 \quad s.t. \quad \mathbf{u} = \mathbf{\Phi}\mathbf{v}, \tag{4.8}$$

which is widely studied in the literature and recently formalized under compressed sensing paradigm.

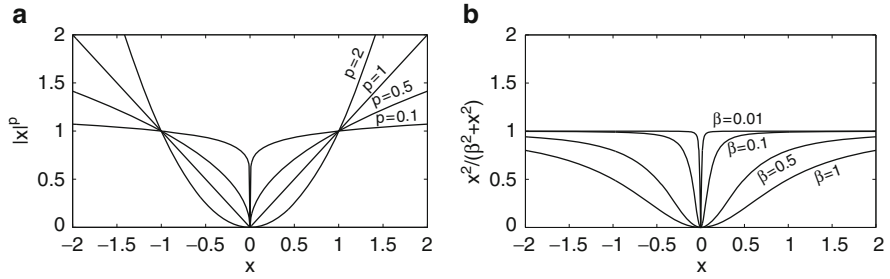

Fig. 4.2 Behavior of $|\mathsf{x}|^p$ for different values of p: (**a**) as $p \to 0$, larger penalties are given to small values of x (the function is convex for $p \geq 1$). (**b**) Behavior of compactness constraint for different values of β and as $\beta \to 0$

For sufficiently sparse solutions when enough measurements are available and the columns of $\mathbf{\Phi}$ are incoherent, the solution to the convex ℓ_1-norm minimization problem is equivalent to the original problem in (P_0). The main advantage of the above convexification over other approximate solution techniques is mainly related to the well-established efficient linear programming techniques (such as interior point method) that can be used to solve the resulting optimization problem (Chen et al. 1998). Several efficient methods have also been recently introduced for solving the (P_1) problem, including *iteratively reweighted least-squares* (Daubechies et al. 2004), *iterated shrinkage algorithms* (Daubechies et al. 2004; Figueiredo and Nowak 2003; Elad et al. 2007), and step-wise algorithms such as *least angle regression* (LARS) (Efron et al. 2004). Some of these greedy-type methods have been applied to the general linear inverse problems in imaging applications (Daubechies et al. 2004, 2008).

4.2.1 Illustrative Example

Let us now consider M direct observations of a parameter field $\mathbf{u}$ with dimension $N = 100$. Under matrix transformation $\mathbf{\Phi}$, the vector $\mathbf{v}$ is a $S = 10$-sparse representation of $\mathbf{u}$. Figure 4.3 displays the compressed sensing solutions for different values of M. As can be verified from this figure, with inadequate observations, the solutions are sparse, match the observed values perfectly, and have smaller ℓ_1-norm than the reference vector. As M increases, it becomes more difficult to match the increased number of measurements without increasing the ℓ_1-norm. At some value of M, perfect reconstruction of the reference model is obtained because no solutions with lower ℓ_1-norm can be found to reproduce the observations. Three observations regarding this example are given as follows. First, replacing ℓ_0-norm with ℓ_1-norm introduces a shrinkage property that, under equal observation match quality, gives preference to solutions with underestimated coefficients. This implies that the shrinkage property can lead to underestimated solutions in realistic problems

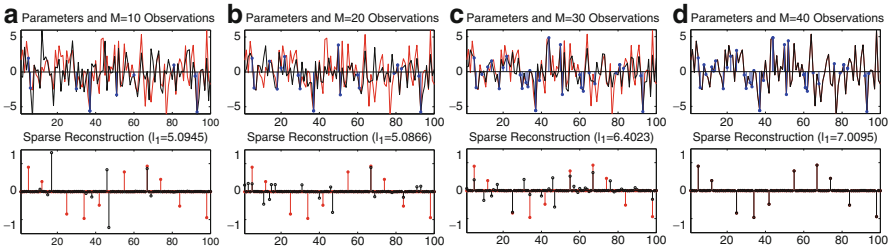

Fig. 4.3 Compressed sensing solution of a simple underdetermined linear system of equations for a $S = 10$-sparse parameter for different values of M; perfect reconstruction is achieved for $M = 40$; *top row* shows the spatial representation of the reference (*red*) and estimated parameters (*black*); the M observed elements are shown with *blue dots*; *bottom row* shows the reference (*red*) and reconstructed (*black*) sparse solutions in the transform domain

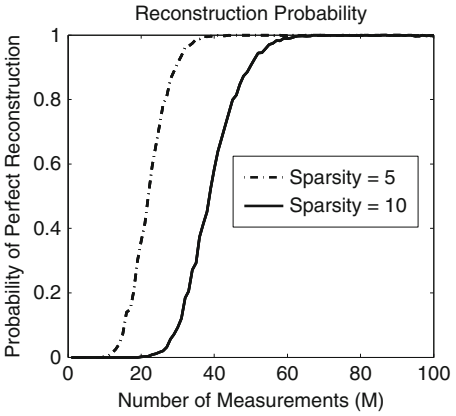

Fig. 4.4 The commutative distribution function (CDF) of perfect reconstruction for a similar example as that shown in Fig. 4.4, but for two cases $S = 5$ and $S = 10$, as a function number of measurements M. The CDF is obtained by repeating the reconstruction for 1,000 times with random measurements and counting the number of times perfect reconstruction was achieved

where perfect reconstruction is impossible due to observations noise. Second, the convex nature of the problem implies that the identified solutions in each case are the global minima. Third, the number of measurements required for perfect reconstruction depends on the specifics of the problem, including the measurement matrix and the measured components of the parameters. For Bernoulli and Gaussian random measurements and sufficiently spare solutions, perfect reconstruction can be achieved with a very high probability for $M > O(S\log(N/S))$. For the example shown in Fig. 4.3, the cumulative probabilities of perfect reconstruction over 1,000 trials with different number of random measurements are shown in Fig. 4.4 for both $S = 5$ and $S = 10$. Perfect reconstruction with smaller number of measurements is possible with lower probability, depending on the measured components.

While compressed sensing provides theoretical guarantees for solving underdetermined linear problems when the solution is sufficiently sparse, such general conditions cannot be specified for nonlinear subsurface flow model calibration problems. Nonetheless, the important guidelines derived from the linear case can be used to facilitate the solution of nonlinear inverse problems. The most remarkable

feature of the above sparsity-promoting algorithms is the selection property of the ℓ_p-norm (for $p \in (0, 1]$) that can identify the significant components of the solution. This norm can be exploited to regularize nonlinear inverse problems where limited observations are used to identify, from a large set of components with potentially many irrelevant elements, a small subset with significant contribution in reproducing the observations. In the next section, typical subsurface flow model calibration is reformulated as a selection problem in which the sparsity-promoting nature of the ℓ_p-norm is invoked to find the solution.

4.3 Sparsity-Promoting Groundwater Model Calibration

To formulate groundwater model calibration as a sparse reconstruction problem, a sparse representation (approximation) of the unknown model parameters must be available. An important step in this direction is to recognize that spatially correlated features often have sparse representations in a properly designed transform domain. In particular, geologic formations are piecewise continuous and exhibit strong spatial correlations. Hence, a proper choice of decorrelating basis functions can be applied to remove the spatial correlation, thereby substantially decreasing the dimension of the parameter field. Such low-dimensional representations give rise to reduced-order approximations that tend to preserve the most salient features of a given geologic model while compromising insignificant details.

4.3.1 Sparse Representations of Aquifer Properties

Physical properties of geologic formations exhibit strong spatial correlations. This strong correlation implies that the underlying physical property maps are amenable to highly sparse or compact representations in a properly designed decorrelating transform domain. *Preconstructed* compression bases and *empirically learned* sparsifying transforms can be used to sparsely represent spatially variable aquifer properties. While generic compressive bases can compactly approximate any given image (property map), they are not as effective as sparse dictionaries that are learned from reliable prior information for a particular application, e.g., subsurface modeling. Sparse geologic dictionaries can be learned from reliable prior training data and are more effective in capturing the expected variability in the formation of interest.

4.3.1.1 Preconstructed (Generic) Sparsifying Transforms

Among notable preconstructed compression transforms are the discrete cosine transform (DCT) that is used in the JPEG image compression (Ahmed et al. 1974;

Britanak et al. 2006) and the discrete wavelet transforms (DWT) that is the basis for the JPEG2000 compression standard (Daubechies 1988; Mallat 2008; Jafarpour 2011). In both methods, the property image is decomposed into its frequency content. For most natural images, after transformation, only a fraction of the basis components have significant contributions to reconstructing the original image, implying that most natural images have sparse approximations in the DCT or DWT domains.

The Discrete Cosine Transform

The DCT is a unitary linear transform that is widely used for image compression because of its well-known near-optimal energy compaction and signal decorrelation power. The one-dimensional forward DCT $v(k), 0 \leq k \leq N-1$, of a signal $\mathbf{u}_N$ of length N and its inverse transform can be expressed as (Britanak et al. 2006)

$$v(k) = \alpha(k) \sum_{n=0}^{N-1} u(n) \cos\left[\frac{\pi(2n+1)k}{2N}\right] \tag{4.9}$$

$$u(n) = \sum_{k=0}^{N-1} \alpha(k) v(k) \cos\left[\frac{\pi(2n+1)k}{2N}\right], \tag{4.10}$$

where $\alpha(k_{1:N-1}) = \sqrt{2}\alpha(0) = \sqrt{\frac{2}{N}}$. The DCT can be interpreted as a real-valued case of the discrete Fourier transform (DFT) and inherits many of the properties of the DFT. For an image with strong spatial correlation, the first few low-frequency modes often adequately explain the main variability in the image. For example, Fig. 4.5a shows the application of the DCT basis in compressing a channelized permeability field. The DCT parameterization has recently been applied to inversion of rock flow properties from flow data (Jafarpour and McLaughlin 2009a,b, 2008). Extension of the DCT to more realistic three-dimensional problems with irregular boundaries and unstructured grid systems is discussed in Bhark et al. (2011).

The Wavelet Transform

A wavelet is a function $\psi(x)$ such that an orthonormal basis of wavelets $\psi_{jk}(x) = 2^{-j/2}\psi(2^{-j}x - k)$ can be generated by dilating and translating this function (Daubechies 1988; Mallat 1989). The idea of the wavelet transform is to represent any measurable, square-integrable 1-D function $f(x) \in L^2(R)$ as a limit of successive approximations, i.e.,

$$f = \sum_{j,k} \langle f, \psi_{jk} \rangle \psi_{jk}. \tag{4.11}$$

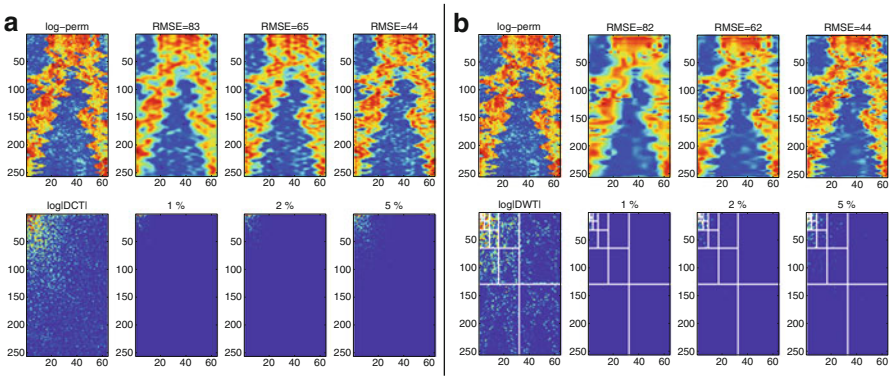

Fig. 4.5 Compression power of the discrete cosine transform (**a**) and the discrete wavelet transform (**b**). In each case, the *first row* shows the spatial representations, while the *second row* displays the transformed coefficients; the *first columns* are related to the original images, while the *remaining columns* show approximations with increasing number of retained coefficients (*left to right*). The number on top of the plots in the second row shows the percentage of coefficients retained in the approximated expansion. The DCT coefficients are usually clustered around the low-frequency basis components (*top-left corner*), and the DWT coefficients have space localization property. Both of these properties will be exploited to incorporate prior information in our sparse reconstruction framework

Moreover, for $j \in [1,2,\ldots]$, $\sum_{k\in\mathbb{Z}}\langle f,\psi_{jk}\rangle\psi_{jk}$ expresses the difference between the approximations of f with resolutions 2^j and 2^{j-1}. This leads to a multiresolution analysis of $L^2(R)$ consisting of a ladder of spaces $\cdots \subset V_2 \subset V_1 \subset V_0 \subset V_{-1} \subset V_{-2} \subset \cdots$ and the existence of a function $\phi \in V_0$ such that $\phi_{0n}(x) = \phi(x-n)$ constitute an orthonormal basis of V_0.

Since ϕ generates a multiresolution analysis, it is called a *scaling function*. The wavelet and scaling functions ψ and ϕ are related by

$$\psi(x) = \sum_{n\in Z}(-1)^n c(-n+1)\phi(2x-n). \tag{4.12}$$

For computation of the *wavelet coefficients*, a convolution followed by a "down-sampling" is performed (Daubechies 1988) $\langle f,\psi_{jk}\rangle$:

$$\langle f,\psi_{jk}\rangle = \sum_n g(n-2k)\langle f,\phi_{j-1n}\rangle,\ \ \langle f,\phi_{jk}\rangle = \sum_n h(n-2k)\langle f,\phi_{j-1n}\rangle, \tag{4.13}$$

where $h(n) = c(n)/\sqrt{2}, g(n) = (-1)^n c(-n+1)/\sqrt{2}$. Similarly, the scaling coefficients are

$$\langle f,\phi_{j-1m}\rangle = \sum_k [h(m-2k)\langle f,\phi_{jk}\rangle + g(m-2k)\langle f,\psi_{jk}\rangle]. \tag{4.14}$$

Compared to Fourier-type methods, the DWT has the benefit of space-frequency localization. This property is seen by comparing the first columns in Fig. 4.5a, b, where, unlike the DCT coefficients, the wavelet coefficients reveal local spatial information about the underlying features in the original spatial map. In inverse problems, this localization benefit may be realized when sufficiently high-resolution data is available to identify and resolve the local features in the solution (Jafarpour 2011). Nonetheless, this spatial localization may be exploited in the inversion to incorporate prior sparse structures and/or to implement adaptive multiresolution inversion.

4.3.1.2 Learned Sparse Geologic Dictionaries

As an alternative to generic compression bases, one can construct application-specific sparse dictionaries from a training database. That is, using a training database as prior knowledge, one can construct a matrix $\mathbf{\Phi}$ such that the projection of the features in the training database onto $\mathbf{\Phi}$ becomes sparse. This approach is widely used in computer vision and object recognition where a training database of a specific object is available (e.g., face or fingerprint features). A learned dictionary is more efficient for reconstructing an object that is similar to those in the training database. In many subsurface characterization applications, such databases can be readily constructed from prior knowledge using geostatistical simulation (Deutsch and Journel 1998).

A relatively simple technique for learning sparse dictionaries from a prior database is the K-SVD algorithm (Kreutz-Delgado et al. 2003; Aharon et al. 2006). Suppose that a database of images containing L samples $\tilde{\mathbf{u}}_{l=1:L}$ is available. Either of the following optimization problems can be solved to find a dictionary that yields a sparse approximation to the samples in the database (Kreutz-Delgado et al. 2003; Aharon et al. 2006):

$$\min_{\mathbf{\Phi},\mathbf{v}_l|_{l=1}^{L}} \|\mathbf{v}_l\|_0 \qquad s.t. \quad \|\tilde{\mathbf{u}}_l - \mathbf{\Phi}\mathbf{v}_l\|_2 \leq \varepsilon, \qquad \text{or} \tag{4.15}$$

$$\min_{\mathbf{\Phi},\mathbf{v}_l|_{l=1}^{L}} \|\tilde{\mathbf{u}}_l - \mathbf{\Phi}\mathbf{v}_l\|_2 \qquad s.t. \quad \|\mathbf{v}_l\|_0 = l_0. \tag{4.16}$$

Although there is no known practical algorithm for efficient solution of these equations, heuristic methods such as the method of directions (MOD) and K-SVD, have been shown to perform reasonably well in finding an empirically learned dictionary (Tropp and Gilbert 2007; Aharon et al. 2006). Unfortunately, the computational complexity of these methods for large-scale problems is considerable. In image processing application this issue is addressed through image segmentation to reduce the dimension of the sparse dictionary.

A main difficulty in using learned dictionaries is that their efficiency depends on the quality and representativeness of the prior database. Generic compression bases such as DWT and DCT may be combined with learned sparse dictionaries to gener-

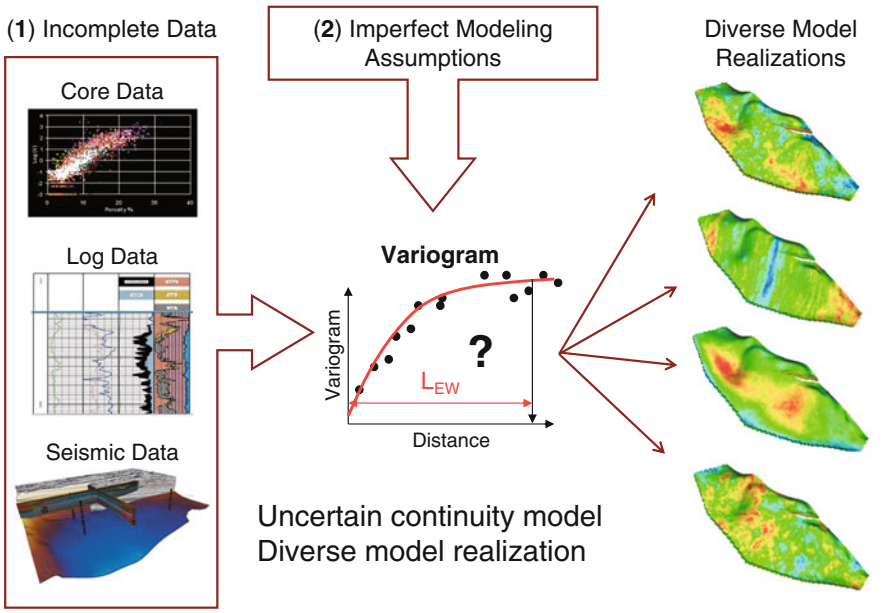

Fig. 4.6 Uncertainty in collected data (**1**) together with imperfect modeling, interpolation, and interpretation assumptions (**2**) can lead to uncertainty in structural continuity model, e.g., variogram. Accounting for uncertainty in structural parameters can result in prior model realizations that have very diverse continuity structure (*right*)

ate hybrid dictionaries that are robust against errors in the prior model (khaninezhad and Jafarpour 2012). When the presumed prior information is incorrect, generic bases with strong compression power are available to approximate the solution of the inverse problem, an important advantage of the hybrid parameterization approach.

4.3.1.3 Sparsity for Identification of Geologic Continuity

The selection property of the sparsity-promoting regularization is the fundamental concept behind sparse inversion algorithms. A sparse reconstruction formulation of an inverse problem is warranted if one expects the solution to be sparse. Sparsifying transforms that were discussed above can be used to justify solution sparsity. Another application in which solution sparsity is expected is when the prior model of geologic continuity (e.g., variogram model) is unknown or uncertain, resulting in very diverse datasets, with many irrelevant content. Figure 4.6 illustrates a scenario where variogram model uncertainty can result in distinctly different model realizations, to the extent that the continuity in most of the realizations becomes irrelevant for reconstruction of the true property distribution. The diversity (uncertainty) in the prior training dataset leads to a geologic dictionary with many

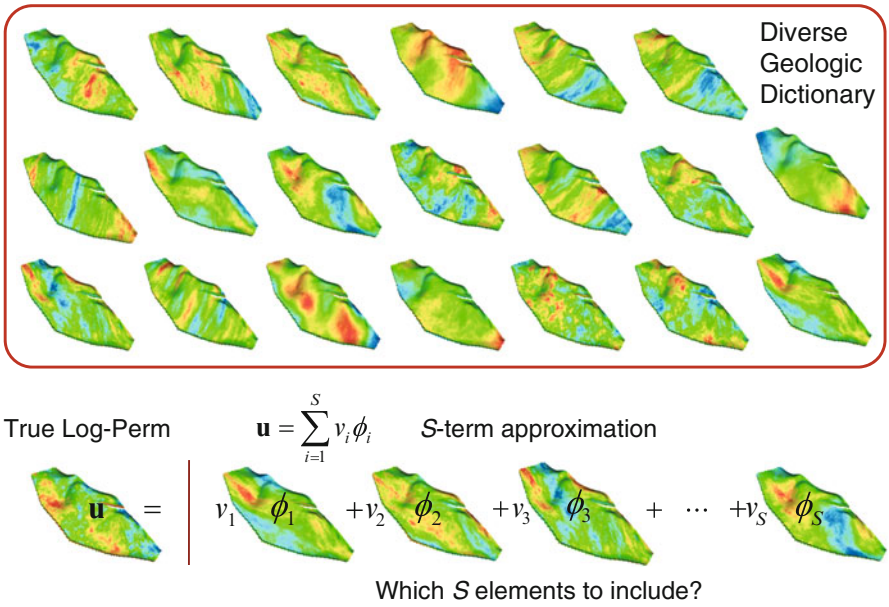

Fig. 4.7 *Top*: diverse geologic dictionaries used to sparsely represent a diverse set of structural continuity in a property field; sparsity is applicable since many of the elements used to represent prior uncertainty are not expected to contribute to the solution. *Bottom*: approximate representation of a reference model as a linear combination of a small subset from the diverse geologic dictionary

elements that have little or no contributions in reconstructing the true solution. As a result, the problem is reduced to selection of very few relevant elements from a diverse geologic dictionary, which can be achieved by sparsity-promoting solution methods. Figure 4.7 shows an example diverse geologic dictionary obtained by treating the variogram model parameters as uncertain random variables. This geologic dictionary can be used to sparsely represent a property field with a given continuity structure.

4.3.2 Sparse Model Calibration Formulation

In groundwater model calibration inverse problems, the relation between measurable quantities (e.g. flow rate and hydraulic head) and unknown parameters (e.g., permeability and porosity) is often nonlinear. While rigorous treatment of the convergence behavior in nonlinear systems is nontrivial, new problem formulation can still be developed to exploit sparsity and regularize the solution. Gradient-based techniques may be used with nonlinear models to search for a sparse solution by minimizing a sparsity-promoting regularized least-squares objective function as discussed next.

4.3.3 Nonlinear Model Calibration Using Sparse Reconstruction

A sparsity-promoting version of the nonlinear inverse problem in (4.3) can be expressed as

$$\min_{\mathbf{v}} J(\mathbf{v}) = \|\mathbf{d}_{\text{obs}} - \mathbf{g}(\mathbf{\Phi v})\|^2_{\mathbf{C}_\mathbf{d}^{-1}} + \gamma^2 \|\mathbf{v}\|_p^p, \tag{4.17}$$

where γ is a regularization parameter, $\mathbf{u} = \mathbf{\Phi v}$, and an ℓ_p-norm approximation to the ℓ_0-norm is used. Since $\mathbf{\Phi}$ is a known dictionary, one can compactly express the problem as

$$\min_{\mathbf{v}} J(\mathbf{v}) = \|\mathbf{d}_{\text{obs}} - \mathbf{g}(\mathbf{v})\|^2_{\mathbf{C}_\mathbf{d}^{-1}} + \gamma^2 \|\mathbf{v}\|_p^p. \tag{4.18}$$

When needed, the relation $\mathbf{u} = \mathbf{\Phi v}$ can be used to readily compute the spatial parameter field (e.g., permeability distribution) $\mathbf{u}$ for any instance (iterate) of $\mathbf{v}$. This formulation of the model calibration inverse problem amounts to finding sufficiently sparse solutions in the linear expansion functions $\mathbf{\Phi}$. Gradient-based optimization methods can be used to solve the above minimization, for example, by using iteratively reweighted least-squares algorithm (Li and Jafarpour 2010). However, care must be exercised when solving this minimization problem since for $p \leq 1$, the derivative of the ℓ_p-norm sparsity-promoting term is not defined for zero components of $\mathbf{v}$, a condition that is given the sparse nature of the solution. A simple practical way to avoid this issue is to place a lower bound on the magnitude of the components of $\mathbf{v}$, i.e., $|v_i| \geq \varepsilon$.

4.3.4 Example Applications of Sparse Reconstruction

4.3.4.1 Example 1: Travel-Time Tomography

Consider a simple straight-ray cross-well tomography example to demonstrate the effectiveness of sparse reconstruction for solving ill-posed subsurface characterization inverse problems. A simple straight-ray cross-well travel-time tomography setup is shown in Fig. 4.8a. A uniformly spaced system of 10 sources is located on the left end of the domain, and a symmetric array of 10 receivers is placed on the right end of the interval. The resulting 100 arrival-time measurements are used to infer the slowness structure of the medium (see Jafarpour and McLaughlin 2009c for additional details). The true slowness used to generate the synthetic inversion data is shown in Fig. 4.8b. Denoting the spatial description of the medium slowness as $\mathbf{u}$ and the travel-time tomography observations as $\mathbf{d}_{\text{obs}}$, the measurement equations for this example can be written as $\mathbf{d}_{\text{obs}100\times1} = \mathbf{\Psi}_{100\times2025}\mathbf{u}_{2025\times1}$. Given the compression property of the DCT basis for correlated spatial images (Jafarpour and McLaughlin 2009a,b), the sparse reconstruction problem can be solved in a

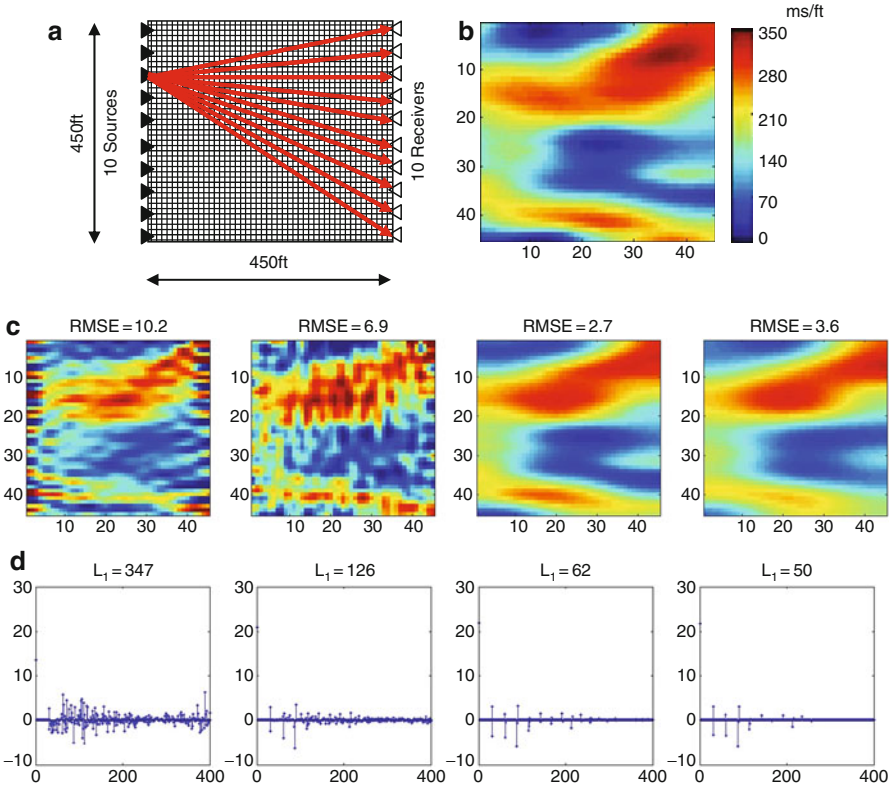

Fig. 4.8 Travel-time tomography example using compressed sensing reconstruction algorithm in a 465-dimensional low-frequency DCT basis: (**a**) experimental setup with 10 transmitters and 10 receivers resulting in a total of 100 measurements, (**b**) reference model with large-scale continuity structure, (**c**) spatial representation of reconstruction results with increasing role of sparsity regularization, and (**d**) reconstructed sparse solution corresponding to the results shown in (**c**)

subspace defined by 465 low-frequency DCT basis components. That is, we write the spatial description of the slowness as $\mathbf{u}_{2025\times 1} = \mathbf{\Omega}_{2025\times 465}\mathbf{v}_{465\times 1}$, where $\mathbf{v}$ stands for the DCT coefficients representing the slowness map and $\mathbf{\Omega}_{2025\times 465}$ denotes the DCT forward transformation matrix (Jafarpour and McLaughlin 2009a,b). For simplicity, the dimension subscripts are dropped hereafter, and the relation between the unknown DCT parameters and arrival-time measurements is expressed as $\mathbf{y} = \mathbf{\Psi u} = \mathbf{\Psi\Omega v}$. Adopting the notation $\mathbf{\Phi} = \mathbf{\Psi\Omega}$, this equation is further simplified to $\mathbf{y} = \mathbf{\Phi v}$. The ℓ_1-norm regularization can now be applied to select and combine the significant DCT components to construct a solution with the best match (in norm-2 sense) to the data. The convex ℓ_1 relaxation sparsity-promoting formulation of the problem can be expressed as

$$\min_{\mathbf{v}} J(\mathbf{v}) = \|\mathbf{u} - \mathbf{\Phi v}\|_2^2 + \gamma^2 \|\mathbf{v}\|_1 . \tag{4.19}$$

In Fig. 4.8c, the spatial representations of the inversion solutions with increasing (from left to right) value of the regularization parameter, γ, are shown. The corresponding DCT coefficients are depicted in Fig. 4.8d. The increasing trend in the regularization parameter (left to right) results in increased sparsity of the solution and in turn relatively larger data mismatches. It can be observed from this example that promoting sparsity in the transform-domain appears to selectively retain the relevant DCT coefficients and estimate their value to match the observed data. It is this selection property of the sparsity penalty that can be exploited to trim irrelevant components that may otherwise remain in the solution and generate artifacts without affecting the data mismatch. When the regularization parameter is too large, the shrinkage property of ℓ_1-norm regularization can lead to solution underestimation (last column of Fig. 4.8c), which is an unintended by-product of approximating ℓ_0-norm with ℓ_1-norm. In our recent publications (Li and Jafarpour 2010; Mohammad-khaninezhad et al. 2012a,b), some of the practical implications of this approximation are discussed, and modified implementations are introduced to mitigate this effect. The above example was used to illustrate how generic transform domain sparse representations of subsurface features can be used to formulate and solve regularized subsurface characterization inverse problems. Next, solution of a nonlinear subsurface flow model calibration inverse problem is presented using geologic dictionaries and a gradient-based minimization method.

4.3.4.2 Example 2: Groundwater Flow Model Calibration

The sparse nonlinear model calibration formulation in Eq. (4.18) is applied to the top layer of the SPE10 model in this section. The model is two-dimensional and has $60 \times 220 = 13,200$ grid blocks. The prior model realizations in this case are constructed using the *sgsim* (Deutsch and Journel 1998) algorithm with highly uncertain variogram model parameters to account for the uncertainty in anisotropy direction. In this case, 3600 realizations are used to construct $K = 500$ K-SVD dictionary elements with a sparsity level of $S = 50$ (10%) (Mohammad-khaninezhad et al. 2012a,b). This implies that all model realizations that are similar to those in the prior library are expected to have S-term approximations in this dictionary. Sample realizations from the prior model are shown in Fig. 4.9a. These realizations have very different continuity structures with many patterns that are not relevant to the reference model. The diverse geologic dictionary is used to reflect the significant level of uncertainty that exists in the direction of continuity in this example. As discussed in Mohammad-khaninezhad et al. (2012a,b), the diversity of the dictionary provides additional support for solution sparsity as many of the dictionary elements will have little or no contribution to the solution. For this example, a two-phase (oil/water) simulation with 13 water injectors and 2 oil producers is considered.

A gradient-based iteratively reweighted algorithm is used to solve the optimization problem. The adjoint method is implemented for efficient computation of the required gradients of the objective function with respect to the permeability

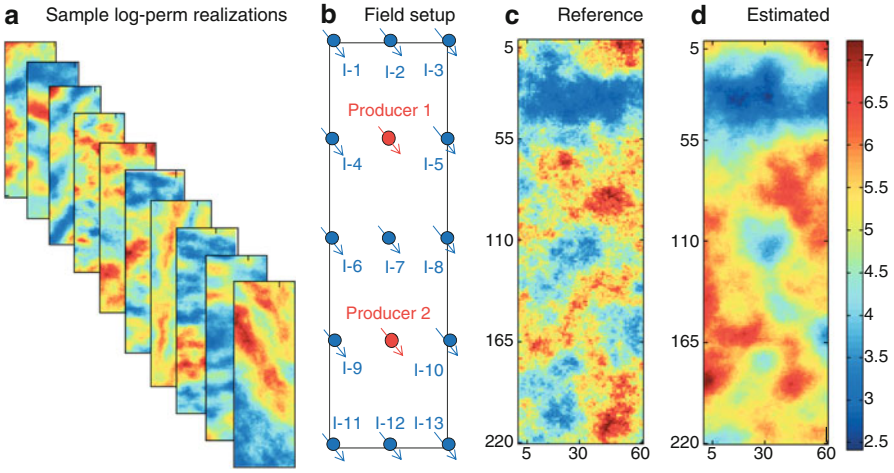

Fig. 4.9 Sparse reconstruction solution of subsurface flow model calibration inverse problem using the top layer of the SPE10 model as an example: (**a**) samples from the initial realizations with diverse continuity structure, (**b**) experimental simulation setup with 15 observation points (wells), (**c**) reference log-permeability field, and (**d**) reconstructed log-permeability model

parameters. Since the permeabilities are linearly related to the K-SVD coefficients ($\mathbf{u} = \mathbf{\Phi v}$), the chain rule of differentiation can be conveniently applied to convert the gradients with respect to the permeability field to the required gradients with respect to the K-SVD coefficients. For brevity, only the final results are presented in here; interested readers are referred to Mohammad-khaninezhad et al. (2012a,b) for additional details about the K-SVD implementation, the problem setup, and the algorithm used to solve the optimization problem. Figure 4.9b shows the well configuration for this example, while Fig. 4.9c depicts the reference log-permeability model. Figure 4.9d displays the log-permeability reconstruction results from dynamic flow measurements collected every 15 days for a total of one year, using the ell_1-norm sparsity-promoting approach. The solution in this case uses a small number of relevant elements from the dictionary to identify the large-scale continuity trends in the reference log-permeability model. The estimated map captures the general permeability trends in the field, with higher accuracy at the vicinity of the observation points (well locations). The performance of the proposed sparsity-promoting model calibration approach is also investigated in several other examples (Jafarpour and McLaughlin 2009c; Jafarpour et al. 2010; Li and Jafarpour 2010; Mohammad-khaninezhad et al. 2012a,b). The preliminary results suggest that sparsity-promoting model calibration methods hold significant potential to improve the solution of ill-posed subsurface model calibration inverse problems. Additional research is underway to explore some of the important properties of this approach and its applicability to realistic field-scale problems.

4.4 Conclusion

A novel subsurface flow model calibration workflow using recent advances in sparse signal processing, known as compressed sensing, was presented. Since its introduction, compressed sensing has received increasing attention in several fields of science and engineering. Here, an overview of the approach and example applications of it were presented. Sparsity is a rich concept and is ubiquitous in subsurface applications. Sparsity-promoting solution of model calibration inverse problems can be achieved by taking advantage of the sparsity in properly designed/selected transform-domain description of aquifer properties (e.g., in DCT and DWT bases and in geologically learned sparse dictionaries). The selection property of the sparsity-promoting inversion implies that the reconstruction results are less sensitive to presence of inconsistent elements in a prior geologic dictionary since these elements are typically given a zero coefficient (contribution) and are removed from the reconstruction. In fact, the diversity of the prior geologic dictionary helps to realize the sparsity of the solution since many of the existing dictionary elements are likely to have little or no contributions to the solution. Overall, sparse model calibration is a promising novel approach for improving the solution of ill-posed subsurface inverse problems that is likely to attract further research attention to develop more effective formulations and efficient implementations algorithms.

References

Aanonsen S (2008) Efficient history matching using a multiscale technique. SPE Reservoir Eval Eng 11(1):154–164

Aharon M, Elad M, Bruckstein A (2006) K-SVD (capitalized): An algorithm for designing overcomplete dictionaries for sparse representation. IEEE Trans Signal Process [see also IEEE Trans Acoust Speech Signal Process] 54(11):4311–4322

Ahmed A, Natarajan T, Rao KR (1974) Discrete cosine transform. IEEE Trans Biomed Eng C23:90–93

Aziz K, Settari A (1979) Petroleum reservoir simulation. Springer, New York

Bear J, Verruijt A (1987) Modeling groundwater flow and pollution (theory and applications of transport in porous media). Applied Science Publishers, London

Bhark E, Jafarpour B, Datta-Gupta A (2011) A generalized grid-connectivity-based parameterization for subsurface flow data assimilation. Water Resour Res 47,W06517:32 PP

Britanak PC, Yip P, Rao K (2007) Discrete cosine transform: general properties, fast algorithms, and integer approximation. Academic Press

Carrera J, Alcolea A, Medina A, Hidalgo J, Slooten LJ (2005) Inverse problem in hydrogeology. Hydrol J 13(1):206–222

Chartrand R, Yin W (2008) Iteratively reweighted algorithms for compressive sensing. IEEE International Conference on Acoustics 2008, Speech and Signal Processing. ICASSP 3869–3872

Chavent G, Bissell R (1998) Indicators for the refinement of parameterization. In: Tanaka M, Dulikravich GS (eds) Inverse Problems in Engineering Mechanics (Proceedings of the International Symposium on Inverse Problems in Engineering Mechanics 1998 (ISIP'98), Nagano, Japan) Elsevier, pp 309–314

Chen SS, Donoho DL, Saunders MA (1998) Atomic decomposition by basis pursuit. SIAM J Sci Comput 20:33–61

Constable S, Parker R, Constable C (1987) Occams inversion: a practical algorithm for generating smooth models from electromagnetic sounding data. Geophysics 52:289–300

Couvreur C, Bresler Y (2000) On the optimality of the backward greedy algorithm for the subset selection problem. SIAM J Matrix Anal Appl 21:797–808

Daubechies I (1988) Multiresolution approximation and wavelet orthonormal bases of $l^2(r)$. Trans Am Math Soc LXI:909–996

Daubechies I, Defrise M, De Mol C (2004) An iterative thresholding algorithm for linear inverse problems with a sparsity constraint. Comm Pure Appl Math 57:1413–1457

Daubechies I, Fornasier M, Loris I (2008) Accelerated projected gradient method for linear inverse problems with sparsity constraints. J Fourier Anal Appl 14,5–6:764–792

Deutsch CV, Journel AG (1998) GSLIB - Geostatistical software library and user's guide. Oxford University Press, New York

Doherty J (2003) Groundwater model calibration using pilot points and regularisation. Ground Water 41(2):170–177

Donoho DL (2006) Compressed sensing. IEEE Trans Inform Theory 52(4):1289–1306

Donoho DL, Elad M (2003) Optimally sparse representation in general (nonorthogonal) dictionaries via l^1 minimization. Proc Natl Acad Sci USA 100(5):2197–2202 (electronic)

Efron B, Hastie T, Johnstine I, Tishirani R (2004) Least angle regression. Ann Stat 32:407–499

Elad M, Matalon B, Zibulevsky M (2007) Coordinate and subspace optimization methods for linear least squares with non-quadratic regularization. Appl Comput Harmonic Anal 23(3):346–367

Figueiredo MAT, Nowak RD (2003) An em algorithm for wavelet-based image restoration. IEEE Trans Image Process 12:906–916

Gavalas GR, Shah PC, Seinfeld JH (1976) Reservoir history matching by bayesian estimation. Soc Petrol Eng J 16(6):337–350

Gorodnitsky IF, Rao BD (1997) Sparse signal reconstruction from limited data using focuss: A re-weighted norm minimization algorithm. IEEE Trans Signal Process 45:600–616

Grimstad AA, Mannseth T, Nvdal G, Urkedal H (2003) Adaptive multiscale permeability estimation. Comput Geosci 7:1–25

Hill MC, Tiedeman CR (2007) Effective groundwater model calibration. Wiley

Jacquard P, Jain C (1965) Permeability distribution from field pressure data. Transactions of the American Institute of Mining, Metallurgical and Petroleum Engineers. (Abbreviated Trans. AIME). Soc Pet Eng J 5(4):281–294

Jafarpour B (2011) Wavelet reconstruction of geologic facies from nonlinear dynamic flow measurements. IEEE Trans Geosci Rem Sens 49(5):1520–1535

Jafarpour B, McLaughlin DB (2008) History-matching with an ensemble kalman filter and discrete cosine parameterization. Comput Geosci 12,2:227–244

Jafarpour B, McLaughlin DB (2009a) Reservoir characterization with discrete cosine transform. part-1: parameterization. SPE Journal, Soc Pet Eng J 14(1):182–201, http://www.onepetro.org/mslib/servlet/onepetropreview?id=SPE-106453-PA

Jafarpour B, McLaughlin DB (2009b) Reservoir characterization with discrete cosine transform. part-2: history matching. SPE Journal, Soc Pet Eng J 14(1):182–201, http://www.onepetro.org/mslib/servlet/onepetropreview?id=SPE-106453-PA

Jafarpour B, Goyal VK, McLaughlin DB, Freeman WT (2009) Transform-domain sparsity regularization for inverse problems in geosciences. Geophysics 74(45):R69–R83, DOI:10.1190/1.3157250

Jafarpour B, Goyal VK, McLaughlin DB, Freeman WT (2010) Compressed history matching: exploiting transform-domain sparsity for regularization of nonlinear dynamic data integration problems. Math Geosci 42:1–27, doi: 10.1007/s11004-009-9247-z

Karlovitz LA (1970) Construction of nearest points in the l_p, p even and l_∞ norms. J Approx Theory 3:123–127

Kitanidis K, Vomvoris EG (1983) A geostatistical approach to the inverse problem in groundwater modeling (steady state) and one-dimensional simulations. Water Resour Res 19(1):677–690

Kreutz-Delgado K, Murray JF, Rao BD, Engan K, Lee TW, Sejnowski TJ (2003) Dictionary learning algorithms for sparse representation. Neural Comput 15(2):349–396

Li L, Jafarpour B (2010) Effective solution of nonlinear subsurface flow inverse problems in sparse bases. Inverse Probl 26(10),105016:24 PP

Mallat S (1989) Multiresolution approximation and wavelet orthonormal bases of $I^2(r)$. Trans Am Math Soc 315:69–88

Mallat S (2009) A wavelet tour of signal processing 3rd edn. Academic Press

Mallat S, Zhang Z (1993) Matching pursuits with time-frequency dictionaries. IEEE Trans Signal Process 41:3397–3415

McLaughlin DB, Townley LR (1996) A reassessment of the groundwater inverse problem. Water Resour Res 32(5):1131–1161

Mohammad-Khaninezhad MR, Jafarpour B, Li L (2012a) Sparse geologic dictionaries for subsurface flow model calibration: Part i. inversion formulation. Adv Water Resour 39:106–121

Mohammad-Khaninezhad MR, Jafarpour B, Li L (2012b) Sparse geologic dictionaries for subsurface flow model calibration: Part ii. robustness to uncertainty. Adv Water Resour 39:122–136

Mohammad-Khaninezhad MR, Jafarpour B (2013) Estimating reservoir connectivity from dynamic data under geologic uncertainty. SPE J (in revision)

Natarajan BK (1995) Sparse approximate solutions to linear systems. SIAM J Comput 24(2):227–234

National Research Council (2000) Seeing into the earth: Noninvasive characterization of the shallow subsurface for environmental and engineering application. Technical report, Washington, DC

Oliver DS, Reynolds AC, Liu N (2008) Inverse theory for petroleum reservoir characterization and history matching. Cambridge University Press, Cambridge

Portniaguine O, Zhdanov MS (1999) Focusing geophysical inversion images. Geophysics 64(3):874–887

Rao BD, Kreutz-Delgado K (2003) An affine scaling methodology for best basis selection. IEEE Trans Signal Process 47:187–200

Sahni I, Horne RN (2005) Multiresolution wavelet analysis for improved reservoir description. SPEREE 8(1):53–69

Santosa F, Symes WW (1986) Linear inversion of band-limited reflection seismograms. SIAM J Sci Stat Comput 7:1307–1330

Tikhonov AN, Arsenin VY (1977) Solution of ill-posed problems. Winston, distributed by Halsted Press, New York

Tonkin M, Doherty J (2005) A hybrid regularized inversion methodology for highly parameterized models. Water Resour Res 41,W10412:170–177

Tropp JA, Gilbert AC (2007) Signal recovery from partial information via orthogonal matching pursuit. IEEE Trans Inf Theory 53:4655–4666

Yeh TCJ, Lee CH, Hsu KC, Illman WA, Barrash W, Cai X, Daniels J, Sudicky E, Wan L, Li G, Winter CL (2008) A view toward the future of subsurface characterization: Cat scanning groundwater basins. Water Resour Res W03301, doi:10.1029/2007WR006375